Journal of Electrical and Computer Engineering Innovations
(JECEI)
Journal homepage: http://www.jecei.sru.ac.ir

Research paper

A Comparative Evaluation of Model Predictive Current Controlled Matrix Converter versus AC-DC-AC Converter

M. Nabizadeh [1], P. Hamedani [2,*], B. Mirzaeian Dehkordi [1]

[1] *Department of Electrical Engineering, University of Isfahan, Isfahan, Iran.*

[2] *Department of Railway Engineering and Transportation Planning, University of Isfahan, Isfahan, Iran.*

Article Info

Article History:
Received 11 November 2024
Reviewed 27 January 2025
Revised 14 February 2025
Accepted 02 March 2025

Keywords:
AC-DC-AC converter
Current control
Matrix converter
Model Predictive Control (MPC)
Weighting factor

*Corresponding Author's Email Address:
p.hamedani@eng.ui.ac.ir

Abstract

Background and Objectives: Due to the disadvantages of the traditional AC-DC-AC converters, especially in electric drive applications, Matrix Converters (MCs) have been widely researched. MCs are well-known structures that remove the DC-Link capacitor and provide bidirectional power flow, while also giving the ability to control reactive power flow, which the AC-DC-AC converter lacks.
Methods: In this work, Model Predictive Current Control (MPCC) is utilized in conjunction with the MC to provide more versatility and controllability than traditional control methods. The work endeavors to investigate the current control of the MC utilizing the finite control set Model Predictive Control (MPC) approach.
Results: Current tracking performance, reactive power control, and switching frequency minimization have been included in the objective function of the controller. Moreover, the results have been compared to the traditional AC-DC-AC converters under similar circumstances. The MC can reduce the switching frequency by 40% compared to the AC-DC-AC converter while maintaining the same current THD value. Additionally, it achieves a 58% reduction in current THD compared to the AC-DC-AC converter at the same average switching frequency. However, in the MC, the mitigation of reactive power and the reduction in switching frequency have opposing effects on the current tracking performance.
Conclusion: This work proposes an MPCC method for the MC with an RL load, effectively controlling load current and reactive power. The reduction of switching commutations was also evaluated using different weighting factors in the prediction strategy for both the MC and AC-DC-AC converters. Simulation results demonstrate that the MC outperforms the AC-DC-AC converter in dynamic response and reactive power control.

Introduction

Nowadays, in multifarious industrial applications, Matrix Converters (MCs) are preferred as a replacement of the traditional AC-DC-AC converters including DC-link capacitors [1]-[4]. Eliminating the DC-link capacitors, results in a more compact, lower weight, and more reliable converter structure [4], [5]. Moreover, the MC has a relatively lower number of switching elements with bidirectional power flow ability [4], [5]. The ability to control the grid-side power factor and produce low distorted input and output waveforms makes MCs attractive for different industrial applications [5].

Since the MC topology was introduced, different methods have been applied to control it [4]. The pulse-width modulation [6], [7] approach and space vector modulation [8], [9] strategies are the two most prevalent approaches used to control the MCs. Moreover, in the control of electrical motor drives fed by MCs, Direct

Torque Control (DTC) has been utilized [10]-[12]. But, in combination with the MC, the mentioned methods are complicated. Other control methods have been proposed for MCs [13]-[16]. However, the main drawback of these control methods is their complexity which makes them unsuitable for industrial applications.

To provide a superior dynamic response and to overcome the complexity in the control of MCs, Model Predictive Control (MPC) was suggested. In addition, MPC is compatible with the system's nonlinear nature and restrictions [17]-[18]. Several works have reviewed the MPC strategy for MCs [17]-[21]. Moreover, in the case of induction motor drives supplied with an MC, different MPC methods have been suggested. The common MPC strategies that have been developed for MCs are Predictive Current Control (PCC) [22]-[24], Predictive Torque Control [25]-[27], Predictive Voltage Control [28]-[29], and Predictive Power Control [30]-[31]. Among them, PCC is the most popular. Different objectives have been considered in the cost function of the PCC, including reactive power [32]-[34], Common-Mode (CM) Voltage [35], switching Losses [36], and efficiency [36]. In [37], the standard weighting factor selection in the objective function is replaced by a fuzzy decision-making strategy, demonstrated through a case study on controlling load and supply currents in a direct matrix converter (DMC). This approach eliminates the need for weighting factors and introduces a simplified selection scheme. However, fuzzy control strategies rely heavily on expert knowledge, making them prone to errors if the rules or membership functions are poorly designed. They can also be computationally demanding in complex systems and lack predictive capabilities, limiting their effectiveness in applications requiring anticipation of future system behavior.

In [38], to mitigate the effects of unbalanced grid voltages, an extended instantaneous power theory generates source current references, ensuring sinusoidal source and balanced output currents. An extended state observer (ESO) eliminates the need for grid voltage sensors by estimating grid voltages and providing delayed voltage information for current reference calculations. However, the ESO is sensitive to model inaccuracies, noise, and parameter variations, which can degrade performance. It also requires precise tuning and adds computational complexity, making real-time implementation challenging in some systems.

Due to the efficacy of the PCC method, this paper concentrates on the MC with the Model Predictive Current Control (MPCC) strategy. Moreover, although many works have studied the MPC of MCs, a comparison between the MC and AC-DC-AC converter with MPCC has not been presented. As a result, this paper investigates the performance of the MPCC strategy for the MC and AC-DC-AC converter. The remainder of this manuscript is structured along these lines: first, the mathematical model of the MC is explained. Then, the MPCC of the MC is described. After that, the simulation results are given for an MC with MPCC and an AC-DC-AC converter with MPCC. Finally, the conclusion is given.

Mathematical Model of an MC

Fig. 1 presents the topology of the three-phase MC. The MC consists of nine bidirectional power electronic switches that supply a three-phase R-L load. The MC is connected to the three-phase power grid using an L-C-R filter (as shown in Fig. 1). The switching condition of each bidirectional power electronic switch is represented by S_{xy}, where x is the source phase ($x \in \{u, v, w\}$) and y is the load phase ($y \in \{a, b, c\}$) (as shown in Fig. 1).

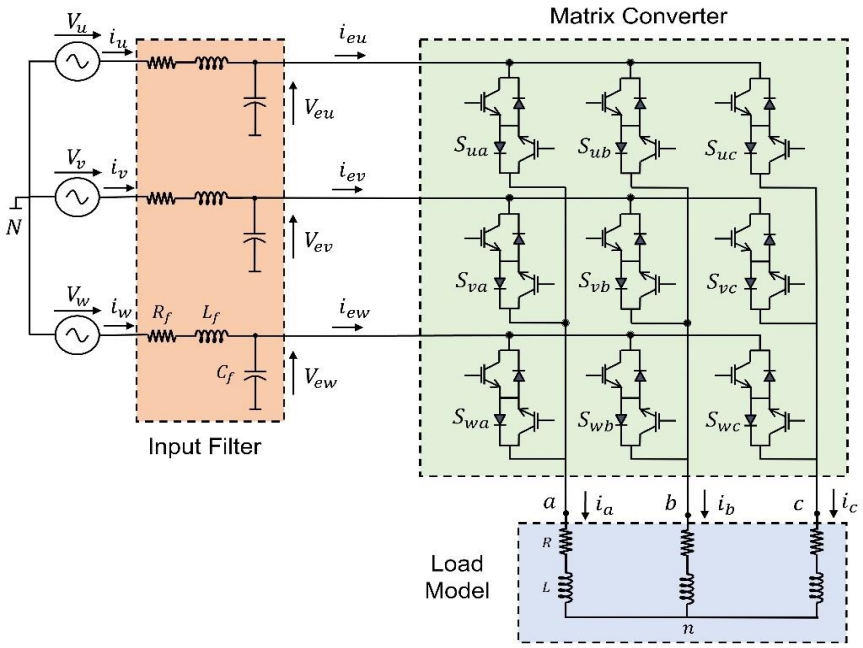

Fig. 1: Topology of a three-phase MC [19].

Note that in the operation of the MC, the short-circuiting of the power source must be avoided by the following restriction [19]:

$$S_{uy} + S_{vy} + S_{wy} = 1 \quad \forall \quad y \in \{a, b, c\} \tag{1}$$

Moreover, in the case of inductive loads, the load current must be continuous to avoid overvoltage in the power electronic elements.

The output voltage of the MC can be derived from the input voltage as follows [21], [22]:

$$\begin{bmatrix} v_{aN}(t) \\ v_{bN}(t) \\ v_{cN}(t) \end{bmatrix} = \underbrace{\begin{bmatrix} S_{ua} & S_{va} & S_{wa} \\ S_{ub} & S_{vb} & S_{wb} \\ S_{uc} & S_{vc} & S_{wc} \end{bmatrix}}_{\boldsymbol{T}} \cdot \begin{bmatrix} v_{eu}(t) \\ v_{ev}(t) \\ v_{ew}(t) \end{bmatrix} \tag{2}$$

or

$$\boldsymbol{v}_o(t) = \boldsymbol{T} \cdot \boldsymbol{v}_e(t) \tag{3}$$

in which $\boldsymbol{T}$ is the transformation matrix and $\boldsymbol{v}_o(k)$ and $\boldsymbol{v}_e(k)$ are the output voltage and input voltage of the MC, respectively:

$$\boldsymbol{v}_o(t) = \begin{bmatrix} v_{aN} \\ v_{bN} \\ v_{cN} \end{bmatrix} \quad and \quad \boldsymbol{v}_e = \begin{bmatrix} v_{eu}(t) \\ v_{ev}(t) \\ v_{ew}(t) \end{bmatrix} \tag{4}$$

Note that the above voltages are written relative to source mid-point N.

The phase voltage relative to the load neutral can be written as [37]:

$$\boldsymbol{v}_{on}(t) = \begin{bmatrix} v_{an} \\ v_{bn} \\ v_{cn} \end{bmatrix} = \begin{bmatrix} v_{aN} - v_{nN} \\ v_{bN} - v_{nN} \\ v_{cN} - v_{nN} \end{bmatrix} \tag{5}$$

v_{nN} can be extracted as [19]:

$$v_{nN} = \frac{v_{aN} + v_{bN} + v_{cN}}{3} \tag{6}$$

where *n* is the neutral point of the load.

The input current can be derived from the output current of the MC as [22]:

$$\begin{bmatrix} i_{eu}(t) \\ i_{ev}(t) \\ i_{ew}(t) \end{bmatrix} = \underbrace{\begin{bmatrix} S_{ua} & S_{ub} & S_{uc} \\ S_{va} & S_{vb} & S_{vc} \\ S_{wa} & S_{wb} & S_{wc} \end{bmatrix}}_{\boldsymbol{T}^T} \cdot \begin{bmatrix} i_a(t) \\ i_b(t) \\ i_c(t) \end{bmatrix} \tag{7}$$

or

$$\boldsymbol{i}_e(t) = \boldsymbol{T}^T \cdot \boldsymbol{i}_o(t) \tag{8}$$

$\boldsymbol{i}_e(k)$ and $\boldsymbol{i}_o(k)$ are the input current of the MC and load current, respectively:

$$\boldsymbol{i}_e(t) = \begin{bmatrix} i_{eu}(t) \\ i_{ev}(t) \\ i_{ew}(t) \end{bmatrix} \quad and \quad \boldsymbol{i}_o(t) = \begin{bmatrix} i_a(t) \\ i_b(t) \\ i_c(t) \end{bmatrix} \tag{9}$$

Using the circuit theory, the input filter state-space model can be derived as [21], [22]:

$$\dot{x}(t) = \underbrace{\begin{bmatrix} 0 & \frac{1}{C_f} \\ -\frac{1}{L_f} & -\frac{R_f}{L_f} \end{bmatrix}}_{\boldsymbol{A_c}} x(t) + \underbrace{\begin{bmatrix} 0 & -\frac{1}{C_f} \\ \frac{1}{L_f} & 0 \end{bmatrix}}_{\boldsymbol{B_c}} u(t) \tag{10}$$

R_f, L_f, and C_f are the filter resistor, inductor, and capacitor, respectively. The state and input vectors are as:

$$\boldsymbol{x}(t) = \begin{bmatrix} \boldsymbol{V}_e(t) \\ \boldsymbol{i}_s(t) \end{bmatrix} \quad and \quad \boldsymbol{u}(t) = \begin{bmatrix} \boldsymbol{V}_s(t) \\ \boldsymbol{i}_e(t) \end{bmatrix} \tag{11}$$

$\boldsymbol{V}_s(t)$ and $\boldsymbol{i}_s(t)$ are the voltage space vector and current space vector at the power supply side, respectively, and can be written as:

$$\boldsymbol{V}_s(t) = 2/3(v_u + \boldsymbol{a}v_v + \boldsymbol{a}^2 v_w) \tag{12}$$

$$\boldsymbol{i}_s(t) = 2/3(i_u + \boldsymbol{a}i_v + \boldsymbol{a}^2 i_w) \tag{13}$$

Using (10), the filter discrete model can be obtained as [39]:

$$\boldsymbol{i}_s(k+1) = \boldsymbol{A}_q(2,1)\,\boldsymbol{V}_e(k) + \boldsymbol{A}_q(2,2)\,\boldsymbol{i}_s(k) + \boldsymbol{B}_q(2,1)\,\boldsymbol{V}_s(k) + \boldsymbol{B}_q(2,2)\,\boldsymbol{i}_e(k) \tag{14}$$

with:

$$\boldsymbol{A}_q = e^{\boldsymbol{A}_c T_s} \quad and \quad \boldsymbol{B}_q = \int_0^{T_s} e^{\boldsymbol{A}_c (T_s - \tau)} \boldsymbol{B}_c d\tau \tag{15}$$

$\boldsymbol{A}_c$ and $\boldsymbol{B}_c$ matrixes can be calculated from (4). T_s is the sampling time.

MPCC of the MC

Fig. 2 illustrates the block diagram of the MPCC for an MC. For all 27 switching conditions of the MC, the load current must be calculated in the next sampling instant. The optimum switching condition for minimizing the objective function is chosen and utilized in the converter in the next sampling instant.

The resistive-inductive load discrete-time model can be written as [40], [41]:

$$\boldsymbol{i}_o(k+1) = \left(1 - \frac{RT_s}{L}\right)\boldsymbol{i}_o(k) + \frac{T_s}{L}(\boldsymbol{v}_{on}(k)) \tag{16}$$

where *k* is the sampling instant. *R* and *L* are the load resistor and inductor, respectively.

$\boldsymbol{v}_{on}(k)$ and $\boldsymbol{i}_o(k)$ are the load phase voltage and load current and can be calculated from (2)-(8).

The general cost function can be written as:

$$g(k+1) = g_i(k+1) + \lambda_Q\, g_Q(k+1) + \lambda_s\, n_{sw}(k+1) \tag{17}$$

where g_i, Q, and n_{sw} are the objective terms regarding the load current, reactive power, and number of switching commutations, respectively. λ_Q *and* λ_S are the weighting factors that adjust the reactive power, and switching commutations, respectively.

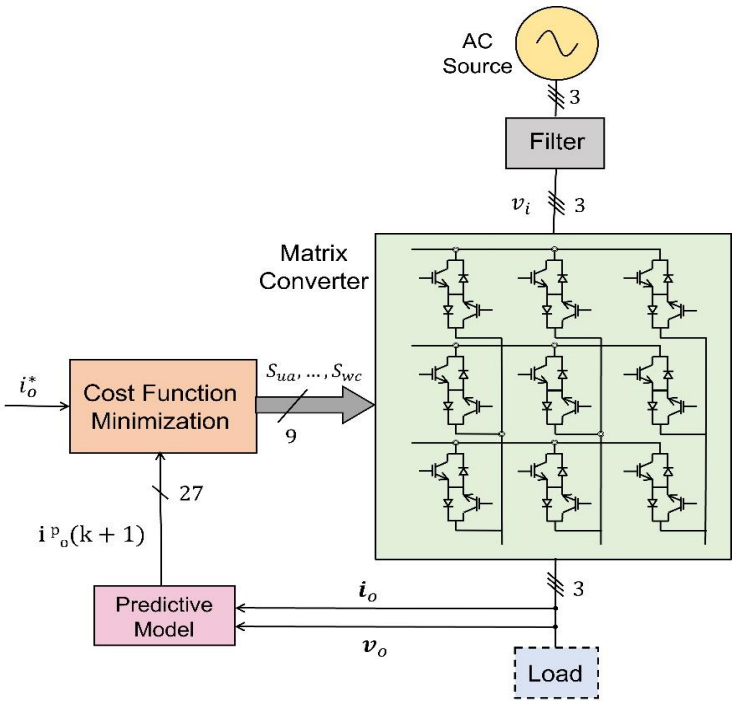

Fig. 2: Diagram of the MPCC for the MC [20].

g_i can be written as [40], [41]:

$$g_i = \left|i^*_{o\alpha}(k+1) - i^p_{o\alpha}(k+1)\right| + \left|i^*_{o\beta}(k+1) - i^p_{o\beta}(k+1)\right| \tag{18}$$

with

$$i_{o\alpha} = \frac{2}{3}\left(i_{oa} - \frac{1}{2}\, i_{ob} - \frac{1}{2}\, i_{oc}\right) \tag{19}$$

$$i_{o\beta} = \frac{2}{3}\left(\frac{\sqrt{3}}{2}\, i_{ob} - \frac{\sqrt{3}}{2}\, i_{oc}\right) \tag{20}$$

Moreover, g_Q can be written as [39]:

$$g_Q = |Q^* - Q(k+1)| \tag{21}$$

in which Q^* is the desired reactive power value. $Q(k+1)$ is the grid-side reactive power and can be computed as [37]:

$$\begin{aligned} Q(k+1) &= Im\{\boldsymbol{V}_s(k+1)\cdot \bar{\boldsymbol{\imath}}_s(k+1)\} \\ &= v_{s\beta}(k+1)\, i_{s\alpha}(k+1) \\ &\quad - v_{s\alpha}(k+1)\, i_{s\beta}(k+1) \end{aligned} \tag{22}$$

In addition, n_{sw} can be defined as [39]:

$$n_{sw}(k+2) = \sum_{x=u,v,w}\ \sum_{y=a,b,c} \left|S_{xy}(k+2) - S_{xy}(k+1)\right| \tag{23}$$

In Fig. 3 the flowchart of the MPCC for an MC is given.

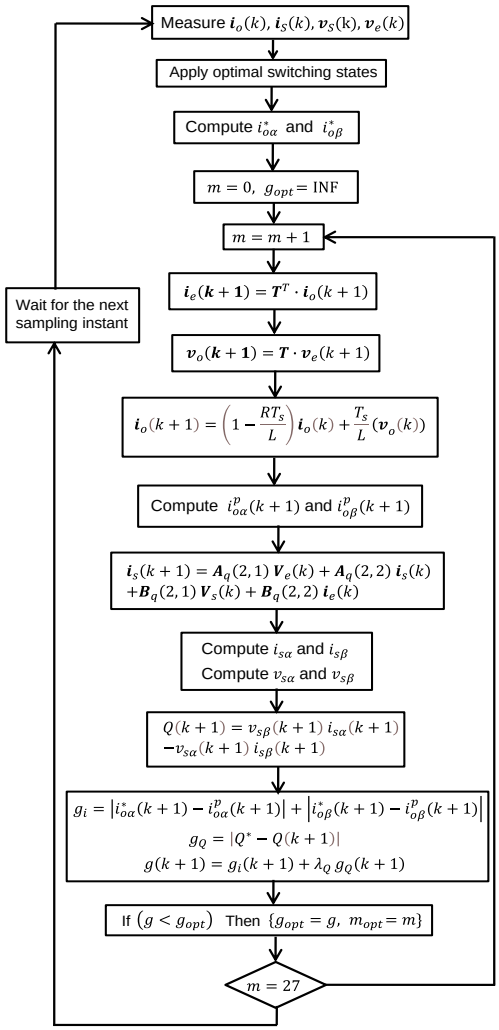

Fig. 3: Flowchart of the MPCC of the MC.

Results and Discussion

The proposed MPCC strategy has been verified by simulating an MC using MATLAB/Simulink. An AC source with a 180 V amplitude and a 50 Hz frequency has been used. The resistance, inductance, and capacitance of the input filter are 0.5 Ω, 400 µH, and 21 µF, respectively. A three-phase load with resistance of 10 Ω and inductance of 30 mH has been used. The sampling time T_s and simulation time-step T_{sim} are 20 µsec and 1 µsec, respectively.

Fig. 4 presents the simulation results of the MC with the MPCC. The weighting factors λ_Q and λ_s are set to zero. The reference currents amplitude is set to 8 A at t=0 sec and is changed from 8 A to 4 A at t=0.1 sec. Fig. 4(a) demonstrates the load current in the MC with the MPCC strategy. The converter has an excellent current tracking performance. Figs. 4(b)-(c) present the phase voltage (V_{an}), and line-to-line voltage (V_{ab}) of the MC with the MPCC method. Fig. 4(d) shows the current of the power supply i_u and the input current of the MC i_{eu}. It is visible that the quality of the power supply current is improved due to the existence of the L-C-R filter. Fig. 4(e) reveals the voltage and current at the power supply side. For λ_Q=0, the input power factor is not controlled. Fig. 4(f) demonstrates the instantaneous reactive power at the power supply side. The reactive power is not controlled.

However, the MC with the MPCC procedure can control the grid-side reactive power. The reactive power at the power supply side can easily be adjusted by increasing the weighting factor λ_Q in the objective function of MPCC.

Fig. 5 shows the simulation results of the MC with MPCC for λ_Q=0.008, indicating an increased weighting factor for the instantaneous grid-side reactive power control parameter in the MPC, compared to Fig. 4.

Fig. 6 presents the simulation results of the MC with MPCC for λ_Q=0.02, the maximum allowable weighting factor for the instantaneous grid-side reactive power control parameter in the MPC, while maintaining the proper current tracking. The parameters used in the simulation are like Fig. 4.

The simulation results demonstrate a significant reduction in the instantaneous grid-side reactive power between the three cases. In Figs. 5-6, where the weighting factor for reactive power control was increased, the system exhibits a marked improvement in minimizing reactive power flow to the grid. This reduction is evident in the smoother and more stable reactive power waveform, which is closer to zero compared to the first simulation. The enhanced control strategy effectively mitigates the fluctuations in reactive power, leading to better overall grid-side power quality and improved system efficiency.

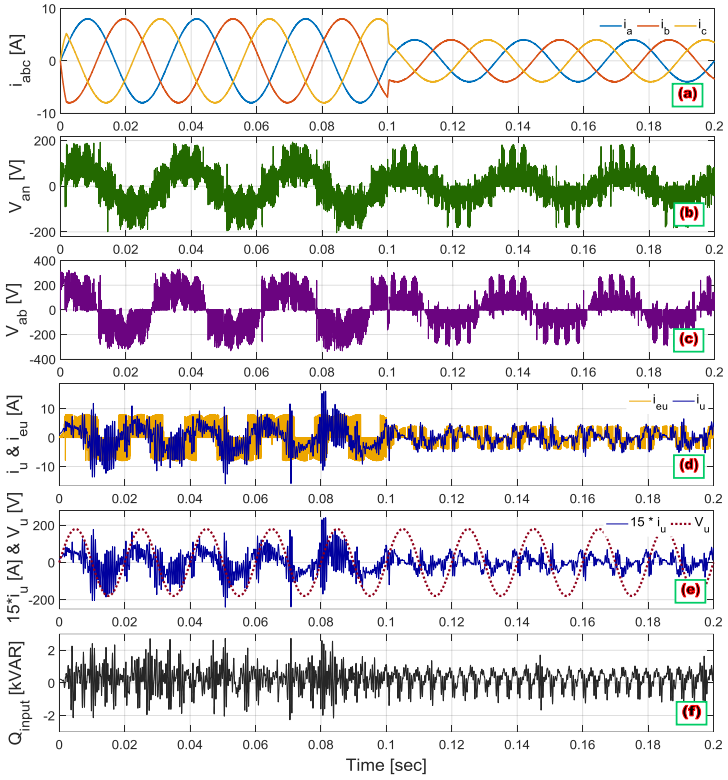

Fig. 4: Simulation results of the MC with MPCC for λ_Q=0: (a) load currents; (b) phase voltage V_{an}; (c) line voltage V_{ab}; (d) i_u and i_{eu}; (e) 15×i_u and V_u voltage; (f) reactive power.

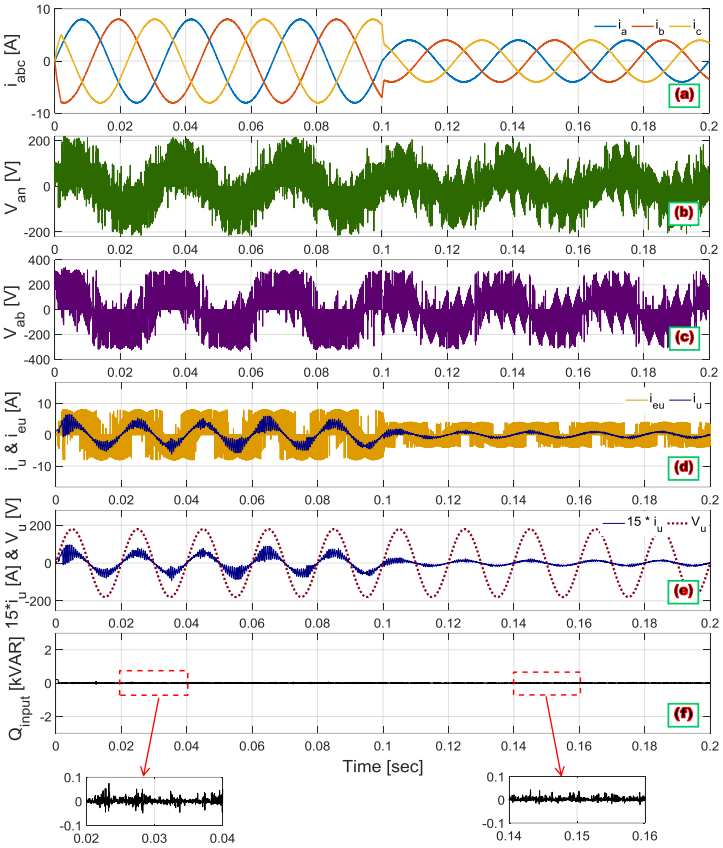

Fig. 5: Simulation results of the MC with MPCC for λ_Q=0.008: (a) load currents; (b) phase voltage V_{an}; (c) line voltage V_{ab}; (d) i_u and i_{eu}; (e) 15×i_u and V_u voltage; (f) reactive power.

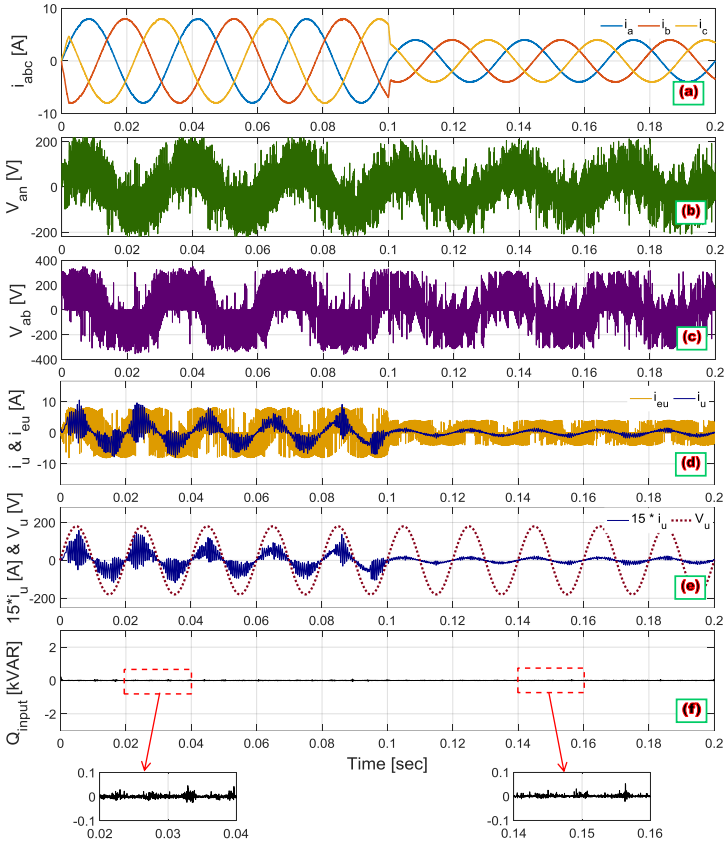

Fig. 6: Simulation results of the MC with MPCC for λ_Q=0.02: (a) load currents; (b) phase voltage V_{an}; (c) line voltage V_{ab}; (d) i_u and i_{eu}; (e) 15×i_u and V_u voltage; (f) reactive power.

In the next part, the behavior of the MC and the AC-DC-AC converter using the MPCC is compared. Fig. 7 illustrates the structure of the AC-DC-AC converter. The simulation parameters of the AC-DC-AC converter are the same as the MC. The DC-link capacitor is C=2 mF in the AC-DC-AC converter. Fig. 8 presents the simulation outcomes in the AC-DC-AC converter with MPCC.

Fig. 8(a) shows the load current in the AC-DC-AC converter with the MPCC method. Figs. 8(b)-(c) present the phase voltage (V_{an}), and line-to-line voltage (V_{ab}) of the AC-DC-AC converter with MPCC method. Fig. 8(d) represents the voltage and current at the power supply side. Fig. 8(e) illustrates the instantaneous power supply side reactive power.

The reactive power is high because the AC-DC-AC converter cannot control it. Moreover, it is visible that the phase and line voltage waveforms as well as the power supply side voltage and current waveforms are more distorted in the AC-DC-AC converter in comparison with the MC.

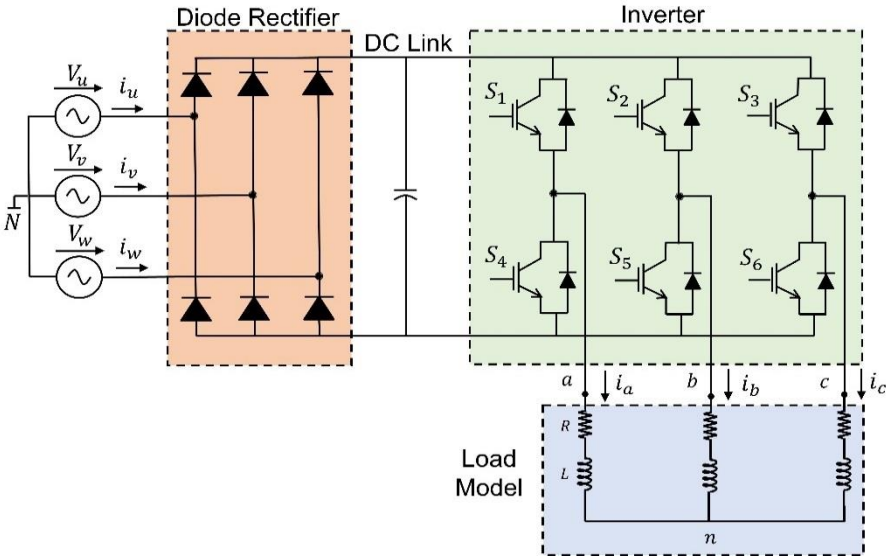

Fig. 7: Structure of the AC-DC-AC converter.

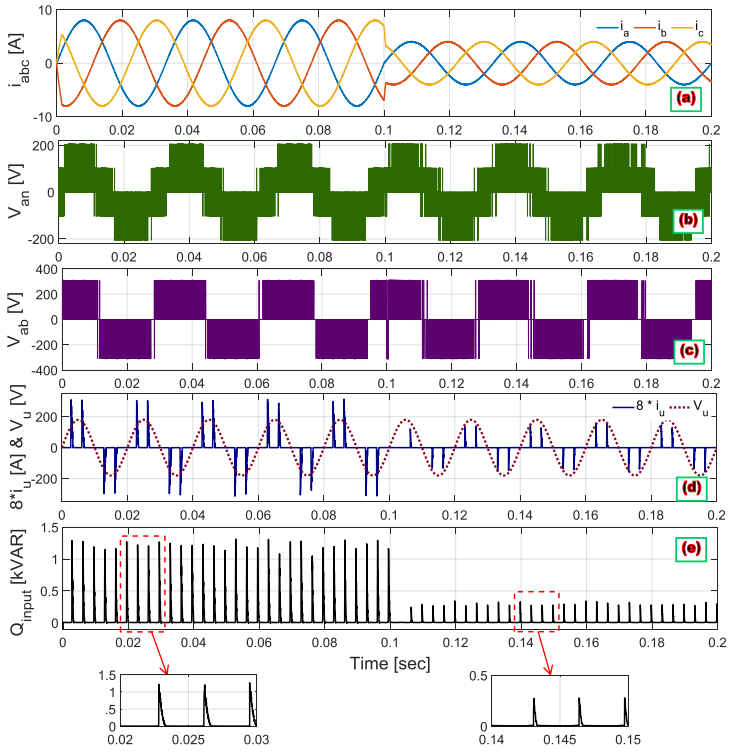

Fig. 8: Simulation results of the AC-DC-AC converter with MPCC: (a) load currents; (b) phase voltage V_{an}; (c) line voltage V_{ab}; (d) 8×i_u and V_u voltage; (e) reactive power.

Table 1 compares the load current THD in the AC-DC-AC converter and MC, both using MPCC. The weighting factor is λ_S=0. The current THD is lower in the MC with λ_Q=0. By increasing λ_Q, the grid-side reactive power of the MC is controlled. Consequently, the tracking performance and THD index of the load current deteriorate. If the reference current amplitude is set to 4 A, the current THD is reduced from 0.983% in the AC-DC-AC converter to 0.594% in the MC, which is a 39.58% reduction. If the reference current amplitude is set to 8 A, the current THD is reduced from 0.458% in the AC-DC-AC converter to 0.318% in the MC, which is a 30.57% decrease.

In the next part, an extra term related to the number of switching commutations is added to the objective function of the MPCC to mitigate the switching frequency of the MC. The system performance and the average switching frequency in the MC have been evaluated with various values of the weighting factor λ_S.

Fig. 9 illustrates the effect of two different values of λ_S on the performance of the MC. The weighting factor λ_Q is set to zero.

The weighting factor λ_S is changed from zero to 0.06 at t=0.05 sec. Figs. 9(a)-(b) show the load current and gate pulse S_{ua} in the MC with MPCC. As can be seen, increasing λ_s mitigates the average switching frequency of the MC from 11.132 kHz to 7.227 kHz. However, it is evident that in higher values of λ_s, there is more current distortion. Note that the switching frequency in Fig. 11 is determined based on the number of switching commutations in a period T for different switches. The average switching frequency of the MC can be calculated as:

$$f_{s-avg} = \frac{1}{9T}\sum_{x=u,v,w}\ \sum_{y=a,b,c} N_{xy} \qquad (24)$$

where N_{xy} is the number of switching commutations for a specific switch, x is the source phase ($x \in \{u, v, w\}$) and y is the load phase ($y \in \{a, b, c\}$).

Fig. 10 presents the effect of two different values of λ_S on the performance of the AC-DC-AC converter. The simulation parameters are the same as Fig. 9. In the AC-DC-AC converter, by increasing λ_s from zero to 0.06, the average switching frequency reduces from 11.205 kHz to 8.39 kHz.

Table 1: Comparison of the load current THD [%] in AC-DC-AC converter and MC with MPCC for λ_S=0

		AC-DC-AC Converter	Matrix Converter		
			λ_Q=0	λ_Q=0.008	λ_Q=0.02
I_{ref} =4 A	Min	0.976	0.578	0.841	0.975
	Max	1.031	0.611	0.911	1.090
	Avg.	0.983	0.594	0.900	1.034
I_{ref} =8 A	Min	0.452	0.300	0.475	0.688
	Max	0.471	0.324	0.526	1.237
	Avg.	0.458	0.318	0.488	0.878

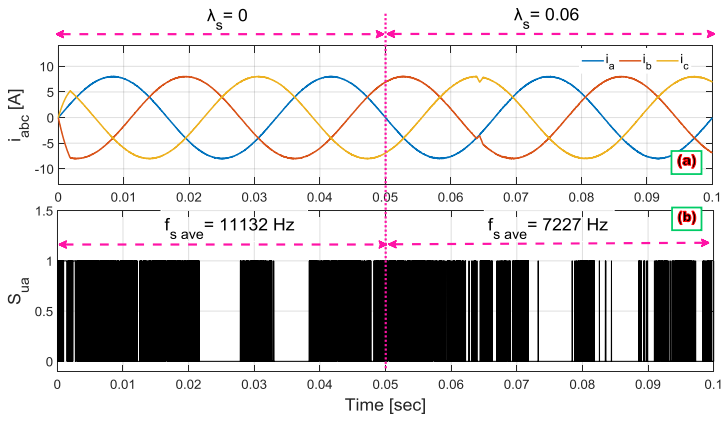

Fig. 9: Impact of λ_s on the performance of the MC: (a) load currents; (b) gate pulse S_{ua}.

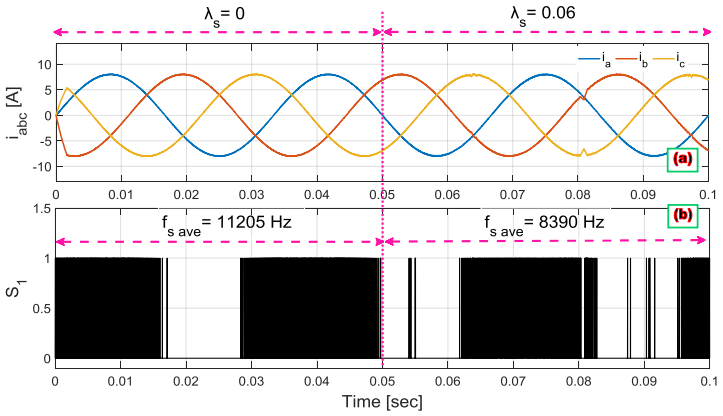

Fig. 10: Impact of λ_s on the behavior of the AC-DC-DC converter: (a) load currents; (b) gate pulse S_1.

Table 2 presents the load current THD of the AC-DC-AC converter and MC with MPCC for and λ_S=0.05.

Fig. 11 compares the current THD versus the average switching frequency in the matrix and AC-DC-AC converters with MPCC. It is visible that for a similar switching frequency, the current THD is lower in the MC compared to the AC-DC-AC converter and vice versa. As an example, at THD=0.48%, the average switching frequency is reduced from 10.4 kHz in the AC-DC-AC converter to 6.5 kHz in the MC. At the average switching frequency of 7 kHz, the THD is reduced from 1.01% in the AC-DC-AC converter to 0.435% in the MC.

Table 2: Comparison of the load current THD [%] in AC-DC-AC converter and MC with MPCC for λ_S=0.05

		AC-DC-AC Converter	Matrix Converter		
			λ_Q=0	λ_Q=0.008	λ_Q=0.02
I_{ref} =4 A	Min	1.246	0.872	1.015	1.133
	Max	1.299	3.082	1.175	1.352
	Avg.	1.277	1.111	1.056	1.187
I_{ref} =8 A	Min	0.589	0.398	0.576	0.800
	Max	0.627	0.455	0.708	1.352
	Avg.	0.617	0.419	0.661	1.187

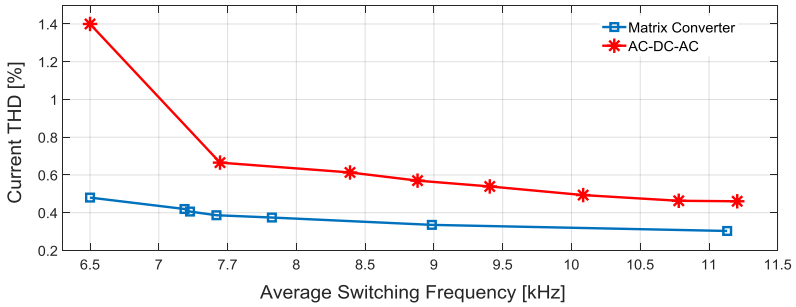

Fig. 11: Current THD versus average switching frequency in MC and AC-DC-AC.

Conclusion

This work has proposed an MPCC method for the MC with an RL load. The suggested method has succeeded in controlling the load current and power supply side reactive power, while other objectives were easily considered in the predictive controller. Additionally, this paper has evaluated the mitigation of the number of switching commutations in the prediction strategy. In this

regard, the prediction control with different weighting factors has been applied to the matrix and the AC-DC-AC converters. Finally, the results of the AC-DC-AC converter and MC were compared. Simulation results have revealed the excellent dynamic response and control of the reactive power at the power supply side in the MC using the MPC approach compared to the traditional AC-DC-AC converter. The AC-DC-AC converter is unable to control the reactive power at the power supply side, but the MC can almost completely mitigate it. The MC can decrease the switching frequency by 40% compared to the AC-DC-AC converter in the same current THD value, and the current THD by 58% compared to the AC-DC-AC converter in the same average switching frequency. However, mitigation of the reactive power and the switching frequency has the opposite effect on the current tracking quality in the MC.

The future work will concentrate on the MPC of motor drives fed by MCs including different objectives in the predictive control process.

Author Contributions

M. Nabizadeh carried out the simulations. Dr. Hamedani was the supervisor and Prof. Mirzaeian Dehkordi was the adviser of the current research paper. Dr. Hamedani wrote the manuscript. All authors revised and discussed the results and approved the final manuscript.

Acknowledgment

The author gratefully acknowledges the respected reviewers and the editor of JECEI for their helpful comments and accurate reviewing of this paper.

Conflict of Interest

The author declares no potential conflict of interest regarding the publication of this work.

Abbreviations

CM	Common-Mode
DTC	Direct Torque Control
MC	Matrix Converter
MPCC	Model Predictive Current Control
MPC	Model Predictive Control
PCC	Predictive Current Control

References

[1] L. Empringham, J. W. Kolar, J. Rodriguez et al., "Technological issues and industrial application of matrix converters: a review," IEEE Trans. Ind. Electron., 60(10): 4260-4271, 2013.

[2] J. Rodriguez, M. Rivera, J. W. Kolar, et al., "A review of control and modulation methods for matrix converters," IEEE Trans. Ind. Electron., 59(1): 58-70, 2012.

[3] S. Muller, U. Ammann, S. Rees, "New time-discrete modulation scheme for matrix converters," IEEE Trans. Ind. Electron., 52(6): 1607-1615, 2005.

[4] P. W. Wheeler, J. Rodriguez, J. C. Clare, L. Empringham, A. Weinstein, "Matrix converters: a technology review," IEEE Trans. Ind. Electron., 49(2): 276-288, 2002.

[5] K. B. Lee, F. Blaabjerg, "Improved sensorless vector control for induction motor drives fed by a matrix converter using nonlinear modeling and disturbance observer," IEEE Trans. Energy Convers., 21(1): 52-59, 2006.

[6] P. G. Potamianos, E. D. Mitronikas, A. N. Safacas, "Open-circuit fault diagnosis for matrix converter drives and remedial operation using carrier based modulation methods," IEEE Trans. Ind. Electron., 61(1): 531-545, 2014.

[7] T. D. Nguyen, H. H. Lee, "Generalized carrier-based PWM method for indirect matrix converters," in Proc. 2012 IEEE Third International Conference on Sustainable Energy Technologies (ICSET): 223-228, 2012.

[8] H. M. Nguyen, H. H. Lee, T. W. Chun, "Input power factor compensation algorithms using a new direct-SVM method for matrix converter," IEEE Trans. Ind. Electron., 58(1): 232-243, 2011.

[9] T. D. Nguyen, H. H. Lee, "A new SVM method for an indirect matrix converter with common-mode voltage reduction," IEEE Trans. Ind. Inf., 10(1): 61-72, 2014.

[10] D. Casadei, G. Serra, A. Tani, "The use of matrix converters in direct torque control of induction machines," IEEE Trans. Ind. Electron., 48(6): 1057-1064, 2002.

[11] H. H. Lee, H. M. Nguyen, T. W. Chun, W. H. Choi, "Implementation of direct torque control method using matrix converter fed induction motor," in Proc. IEEE International Forum on Strategic Technology: 51-55, 2007.

[12] H. Dan, P. Zeng, W. Xiong, M. Wen, M. Su, M. Rivera, "Model predictive control-based direct torque control for matrix converter-fed induction motor with reduced torque ripple," CES Trans. Electr. Mach. Syst., 5(2): 90-99, 2021.

[13] J. Monteiro, J. F. Silva, S. F. Pinto et al., "Matrix converter-based unified power-flow controllers: advanced direct power control method," IEEE Trans. Power Deliv., 26(1): 420-430, 2011.

[14] X. Wang, Q. Guan, L. Tian, "A novel adaptive fuzzy control for output voltage of matrix converter," in Proc. IEEE Power Electronics and Motion Control Conference (IPEMC): 53-58, 2012.

[15] C. F. Calvillo, F. Martell, J. L. Elizondo et al., "Rotor current fuzzy control of a DFIG with an indirect matrix converter," in Proc. IEEE Industrial Electronics Society (IECON): 4296-4301, 2011.

[16] T. S. Sivarani, S. J. Jawhar, C. A. Kumar, "Novel intelligent hybrid techniques for speed control of electric drives fed by matrix converter," in Proc. IEEE Computing, Electronics and Electrical Technologies (ICCEET): 466-471, 2012.

[17] M. Rivera, P. Wheeler, A. Olloqui, D. Khaburi, "A review of predictive control techniques for matrix converters—Part I," in Proc. IEEE Power Electronics and Drive Systems Technologies Conference (PEDSTC): 582-588, 2016.

[18] M. Rivera, P. Wheeler, A. Olloqui, "Predictive control in matrix converters—Part II: Control strategies, weaknesses and trends," in Proc. IEEE International Conference on Industrial Technology (ICIT): 1098-1104, 2016.

[19] S. Toledo, D. Caballero, E. Maqueda, J. J. Cáceres, M. Rivera, R. Gregor, P. Wheeler, "Predictive control applied to matrix converters: A systematic literature review," Energies, 15(20): 7801, 2022.

[20] M. Khosravi, M. Amirbande, D.A. Khaburi, M. Rivera, J. Riveros, J. Rodriguez, A. Vahedi, P. Wheeler, "Review of model predictive control strategies for matrix converters", IET power Electron., 12(12): 3021-3032, 2019.

[21] R. Vargas, J. Rodriguez, C. A. Rojas, M. Rivera, "Predictive control of an induction machine fed by a matrix converter with increased efficiency and reduced common-mode voltage," IEEE Trans. Energy Convers., 29(2): 473-485, 2014.

[22] R. Vargas, J. Rodriguez, U. Ammann, P. W. Wheeler, "Predictive current control of an induction machine fed by a matrix converter

with reactive power control," IEEE Trans. Ind. Electron., 55(12): 4362-4371, 2008.

[23] L. Tarisciotti et al., "Modulated predictive control for indirect matrix converter," IEEE Trans. Ind. Appl., 53(5): 4644-4654, 2017.

[24] Y. Liu, Y. Liu, B. Ge, H. Abu-Rub, "Interactive grid interfacing system by matrix-converter-based solid state transformer with model predictive control," IEEE Trans. Ind. Inf., 16(4): 2533-2541, 2020.

[25] J. Rodriguez, R. Pontt, R. Vargas et al., "Predictive direct torque control of an induction motor fed by a matrix converter," in Proc. IEEE European Conference on Power Electronics and Applications: 1-10, 2007.

[26] M. López, J. Rodriguez, C. Silva, M. Rivera, "Predictive torque control of a multidrive system fed by a dual indirect matrix converter," IEEE Trans. Ind. Electron., 62(5): 2731-2741, 2015.

[27] M. Uddin, S. Mekhilef, M. Mubin, M. Rivera, J. Rodriguez, "Model predictive torque ripple reduction with weighting factor optimization fed by an indirect matrix converter," Electr. Power Compon. Syst., 42(10): 1059-1069, 2014.

[28] S. Toledo et al., "Active and reactive power control based on an inner predictive voltage control loop for AC generation systems with direct matrix converter," in Proc. IEEE International Autumn Meeting on Power, Electronics and Computing (ROPEC): 1-6, 2019.

[29] S. Toledo et al., "Active and reactive power control based on predictive voltage control in a six-phase generation system using modular matrix converters," in Proc. IEEE International Conference on Industrial Technology (ICIT): 1059-1065, 2020.

[30] M. Ortega, F. Jurado, J. Carpio, "Control of indirect matrix converter with bidirectional output stage for micro-turbine," IET Power Electron., 5(6): 659-668, 2012.

[31] S. Yusoff, L. De Lillo, P. Zanchetta, P. Wheeler, "Predictive control of a direct AC/AC matrix converter power supply under non-linear load conditions," in Proc. IEEE International Power Electronics and Motion Control Conference (EPE/PEMC): DS3c.4-1-DS3c.4-6, 2012.

[32] M. Rivera, J. Rodriguez, J. R. Espinoza, H. Abu-Rub, "Instantaneous reactive power minimization and current control for an indirect matrix converter under a distorted AC supply," IEEE Trans. Ind. Inf., 8(3): 482-490, 2012.

[33] C. F. Garcia, M. E. Rivera, J. R. Rodríguez, P. W. Wheeler, R. S. Peña, "Predictive current control with instantaneous reactive power minimization for a four-leg indirect matrix converter," IEEE Trans. Ind. Electron., 64(2): 922-929, 2017.

[34] M. Roostaee, B. Eskandari, M. R. Azizi, "Predictive current control with modification of instantaneous reactive power minimization for direct matrix converter," in Proc. IEEE Power Electronics, Drives Systems and Technologies Conference (PEDSTC): 199-205, 2018.

[35] M. Rivera, J. Rodriguez, J. Espinoza, B. Wu, "Reduction of common-mode voltage in an indirect matrix converter with imposed sinusoidal input/output waveforms," in Proc. IEEE Industrial Electronics Society Conference (IECON 2012): 6105-6110, 2012.

[36] R. Vargas, U. Ammann and J. Rodriguez, "Predictive Approach to Increase Efficiency and Reduce Switching Losses on Matrix Converters," IEEE Transactions on Power Electronics, 24(4): 894-902, 2009.

[37] F. Villarroel, J. Espinoza, C. Rojas, C.; Molina, E. A. Espinosa, "multiobjective ranking based finite states model predictive control scheme applied to a direct matrix converter," in Proc. IECON Proceedings (Industrial Electronics Conference): 2941-2946, 2010.

[38] W. Xiong, Y. Sun, J. Lin, M. Su, H. Dan, M. Rivera, J. M. Guerrero, "A cost-effective and low-complexity predictive control for matrix converters under unbalanced grid voltage conditions," IEEE Access, 7: 43895-43905, 2019.

[39] J. Rodriguez, P. Cortes, Predictive control of power converters and electrical drives, John Wiley & Sons, 2012.

[40] P. Hamedani, M. Changizian, "A new hybrid predictive-pwm control for flying capacitor multilevel inverter," J. Electr. Comput. Eng. Innovations (JECEI), 12(2): 353-362, 2024.

[41] P. Hamedani, "Multistep model predictive control of diode-clamped multilevel inverter," J. Electr. Comput. Eng. Innovations (JECEI), 13(1): 117-128, 2025.

Biography

Matin Nabizadeh was born in Kerman, Iran, in 2000. He received the B.Sc. degree in Electrical Engineering from University of Isfahan, Iran, in 2022. He is currently a M.Sc. student in Electrical Engineering in University of Isfahan. His research interests include power electronics and motor drives, intelligent systems, and renewable energy

- Email: m.nabizadeh@eng.ui.ac.ir
- ORCID: 0009-0009-8641-7336
- Web of Science Researcher ID: NA
- Scopus Author ID: NA
- Homepage: NA

Pegah Hamedani was born in Isfahan, Iran, in 1985. She received B.Sc. and M.Sc. degrees from University of Isfahan, Iran, in 2007 and 2009, respectively, and the Ph.D. degree from Iran University of Science and Technology, Tehran, in 2016, all in Electrical Engineering. Her research interests include power electronics, control of electrical motor drives, supply system of the electric railway (AC and DC), linear motors & MAGLEVs, and analysis of overhead contact systems. She is currently an Assistant Professor with the Department of Railway Engineering and Transportation Planning, University of Isfahan, Isfahan, Iran. Dr. Hamedani was the recipient of the IEEE 11th Power Electronics, Drive Systems, and Technologies Conference (PEDSTC'20) best paper award in 2020.

- Email: p.hamedani@eng.ui.ac.ir
- ORCID: 0000-0002-5456-1255
- Web of Science Researcher ID: AAN-2662-2021
- Scopus Author ID: 37118674000
- Homepage: https://engold.ui.ac.ir/~p.hamedani/

Behzad Mirzaeian Dehkordi was born in Shahrekord, Iran, in 1966. He received the B.Sc. degree in Electronics Engineering from Shiraz University, Iran, in 1985, and the M.Sc. and Ph.D. degrees in Power Engineering from the Isfahan University of Technology (IUT), in 1994 and 2000, respectively. In September 2002, he joined the Department of Electrical Engineering, University of Isfahan, where he is currently a Professor of Electrical Engineering. He was a Visiting Professor with the Power Electronic Laboratory, Seoul National University (SNU), South Korea, from March 2008 to August 2016. His research interests include power electronics and motor drives, intelligent systems, and renewable energy

- Email: mirzaeian@eng.ui.ac.ir
- ORCID: 0000-0002-1124-8138
- Web of Science Researcher ID: NA
- Scopus Author ID: NA
- Homepage: https://engold.ui.ac.ir/~mirzaeian/

How to cite this paper:
M. Nabizadeh, P. Hamedani, B. Mirzaeian Dehkordi, "A comparative evaluation of model predictive current controlled matrix converter versus AC-DC-AC converter," J. Electr. Comput. Eng. Innovations, 13(2): 431-442, 2025.

DOI: 10.22061/jecei.2025.11435.804

URL: https://jecei.sru.ac.ir/article_2304.html